

Geological Investigation of Clay Minerals Swelling at the Ciurug, Pongkor Gold-Silver Deposit, West Java, Indonesia

Even Gevor, I Gde Budi Indrawan*, and I Wayan Warmada

Department of Geological Engineering, Faculty of Engineering, Universitas Gadjah Mada, Yogyakarta, Indonesia

Received: June 26, 2024 | Accepted: September, 2024 | Published online: October 31, 2024

ABSTRACT. In underground mining, one of the most important aspects is the technical aspect. Technical aspects Clay minerals that have special behavior in the form of development include the smectite group (montmorillonite, saponite, beidelite, and others). This can also be caused by the argillic zone at the underground tunnel location in Unfoloader 600 and XC Loop 2 Ciurug. The argillic process that causes actual material development in the field weakens the rock mass around the mining development area. The cross-cut location of the Unfoloader 600 and XC Loop 2 tunnels contains active clay minerals with a high percentage of development mineral material composition. The Unfoloader 600 location has a development mineral composition of 102.94 % within 24 hours, indicating very high development potential. Minerals based on XRD testing are illite, kaolinite, and montmorillonite. The XC Loop 2 location has a development mineral composition of 131.25 % within 24 hours, indicating very high development potential. Based on XRD testing, minerals include illite, kaolinite, quartz, and montmorillonite. The values obtained from the free-swelling test in the laboratory and XRD indicate that the location experienced deformation and swelling of rocks in the mining development area.

Keywords: Rock deformation · Swelling · Clay minerals · Argillic zone · Pongkor.

1 INTRODUCTION

In certain cases, tunnel engineering activities can produce many damaging effects, such as the rise of the tunnel floor and the destruction and deformation of the primary and permanent support system (Butcher *et al.*, 2011). Clay minerals that experience free swelling in the soil are determined by the volume change ratio from dry to wet (Nelson *et al.*, 2015). Material swelling occurs due to structural changes in the moisture content of materials containing clay minerals (Wesley, 2010). Clay minerals that experience free swelling are classified as smectite minerals (montmorillonite, smectite, illite, etc.). The presence of these minerals needs to be

closely monitored, especially in underground mining.

Argillic alterations can be defined by montmorillonite, illite, chlorite, kaolin group minerals (kaolinite and halloysite), and a small amount of sericite. K-feldspar might be partially replaced, and K, Ca, Mg, and Na are not entirely leached (Pirajno, 2009). Previous researchers, such as Ginanjar and Sadisun (2019), explained the estimated condition of swelling materials and conducted XRD testing to determine active clay minerals. Based on the conditions at the research site of XC Loop 2 and Unfoloader 600 Ciurug, the effects of rock deformation with poor conditions were found, and active clay minerals such as montmorillonite, saponite, and beidellite were identified. These minerals have the potential to cause a collapse in the tunnel.

*Corresponding author: I G.B. INDRAWAN, Department of Geological Engineering, Universitas Gadjah Mada. Jl. Grafika 2 Yogyakarta, Indonesia. E-mail: igbindrawan@ugm.ac.id

2 GEOLOGICAL SETTING/SITE CHARACTERIZATION

The Pongkor region is part of the Neogene Sunda Banda continental arc that developed along the southern side of the Eurasian Plate due to the subduction of the Indian-Australian Plate. The geological unit is located on land about 40 to 80 km, including shale and basement sandstone overlain by the center of the volcanic belt from the Oligocene to the early Miocene, consisting of mostly volcanic rocks interspersed with limestone and sandstone (Figure 1). Intermediate intrusive rocks are included in the formation with Paleogene and Early Miocene ages. (Basuki, 1994 in Warmada *et al.*, 2003). The types of rocks in the research area are Tuff, Breccia, and Andesite.

Observations were made by collecting data at the Ciurug mine road tunnel access location level 600 in the underground mine of PT. Antam Pongkor, West Java, has a Northwest-Southeast direction, with an entrance in the Southeast (Figure 2). The location that is the object of this study consists of two faces of the tunnel road opening, namely Unfoloader 600 Ciurug and XC Loop 2 Ciurug. The Unfoloader 600 location has an elevation of 610 meters above sea level with a distance from the exit of 187.63 meters, and XC Loop 2 Ciurug has an elevation of 670 meters above sea level with a distance from the entrance of 465.43 meters.

3 METHODOLOGY

The research method that was carried out in this study consisted of introduction, data collection, and data analysis. The materials in this study included regional and local geological maps and rock samples. Samples taken directly in the field include (Tuff, Breccia, and Andesite). The analysis carried out in this study is tunnel mapping to determine rock distribution, geological structure petrography to determine mineral composition, and XRD to obtain swelling mineral composition.

3.1 Free swelling test

Several factors can influence the stability of underground holes (Hoek and Brown, 1982), that:

- Geological structure
- High in-situ stress on rock mass.

- Weathering or swelling in rocks.
- The existence of soil flows.

Free swelling testing is conducted to estimate () Free Swell Index Values (Nelson *et al.*, 2015). The Free Swell Index (%) is the indirect expansion potential of expansive soil. The calculation of the free swell index value (Nelson *et al.*, 2015) is determined using the following formula:

$$FSI = \frac{v_d - v_s}{v_k} \times 100 \quad (1)$$

Where, v_d is defined as the volume of soil samples read from a measuring cup containing distilled water (ml), and notation v_k is defined as the volume of soil samples read from a measuring cup containing tang/kerosene oil (ml).

TABLE 1. Expansion potential based on free swell index value (Nelson *et al.*, 2015).

Free Swell Index (%)	Swell Potential
<20	Low
20-35	Medium
35-50	High
>50	Very High

Samples obtained at PT. Antam Pongkor was used to estimate the potential expansion when in contact with water. To assess the potential development process of rocks and soils, it is essential to make a correlation from the XRD data plotted in (Figure 3) regarding the potential for free swelling (Barla, 1999). All tests were performed on material finer than 4.75 mm (No. 4 sieve). The clay size fraction (CSF) represents the percentage of material finer than 2 μm as determined by hydrometer analysis (Ashayeri and Yasrebi, 2009).

Figure 3 illustrates a strain-time plot depicting constant fluctuations in strain for 48 or 24 hours during the free swelling test (Bayati *et al.*, 2021). Various factors, including soil composition and environmental conditions, influence swelling conditions, necessitating the correlation between clay content and Atterberg Limits (Seed *et al.*, 1962).

3.2 X-ray diffraction test

XRD analysis is employed to characterize XRD (X-ray diffraction) testing conducted on chemical compounds or solid rocks using X-ray reflections. X-rays are electromagnetic radiation

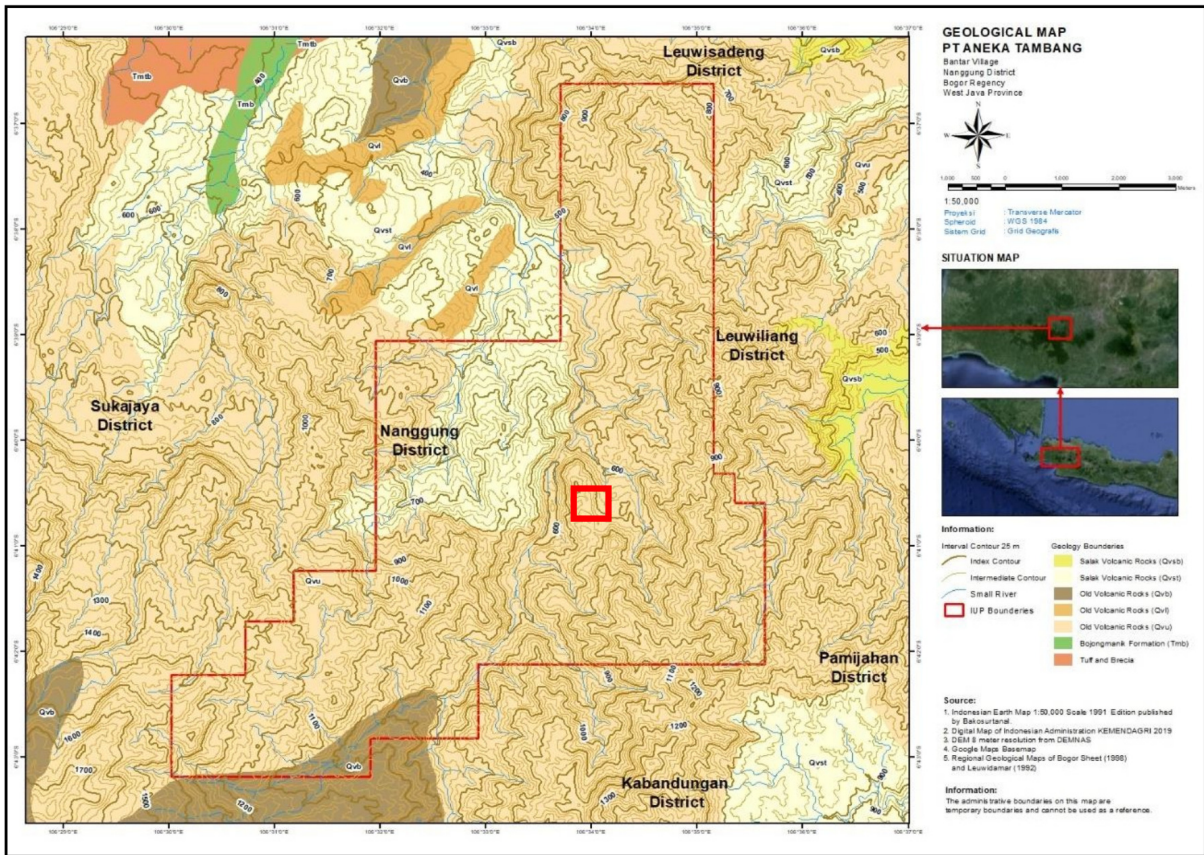


FIGURE 1. Regional Geological Map (Modified from Effendi *et al.*, 1998).

produced by the abrupt deceleration of high-speed particles (Wicaksono *et al.*, 2017). Bragg’s law governs the fundamental principle in X-ray diffraction (Bunaciu *et al.*, 2015).

$$n\lambda = 2d \sin \theta \quad (2)$$

Where, n is an integer, λ is the X-ray wavelength, d is the interplanar distance to the diffraction product, and θ is the diffraction angle.

In the laboratory, XRD tests are utilized to analyze the mineralogy of rock and soil samples. Laboratory observations revealed that all samples contained calcite, quartz, and clay minerals. Test samples contain at least 10 % illite minerals, indicating a moderate development potential, albeit lower than montmorillonite (Bayati *et al.*, 2021).

Reflection XRD 001 modeling simulation to analyze behavior in swelling conditions. The correlation between XRD results and swelling agrees with experiments on homogeneity, smectite hydration, changes in distance be-

tween layers, domain size, and distribution between layers dl (Reynolds and Hower, 1970).

XRD (X-ray diffraction) testing was conducted to further validate the presence of clay minerals in samples from two mining development areas: Unfoloader 600 Ciurug and XC Loop 2 Ciurug. Identifying clay minerals influenced by hydrothermal alteration processes was performed through bulk sample XRD analysis at these two research locations.

4 RESULTS AND DISCUSSION

Based on the conditions at the research location of the XC Loop 2 and Unfoloader 600 Ciurug tools, 3 types of rock lithology were found, namely tuff, breccia, and andesite (Figure 4). The location of the observation area has the influence of rock deformation with poor conditions, so active clay minerals were found in the form of (montmorillonite, saponite, beidelite, and others) which have the potential to cause tunnel collapse.

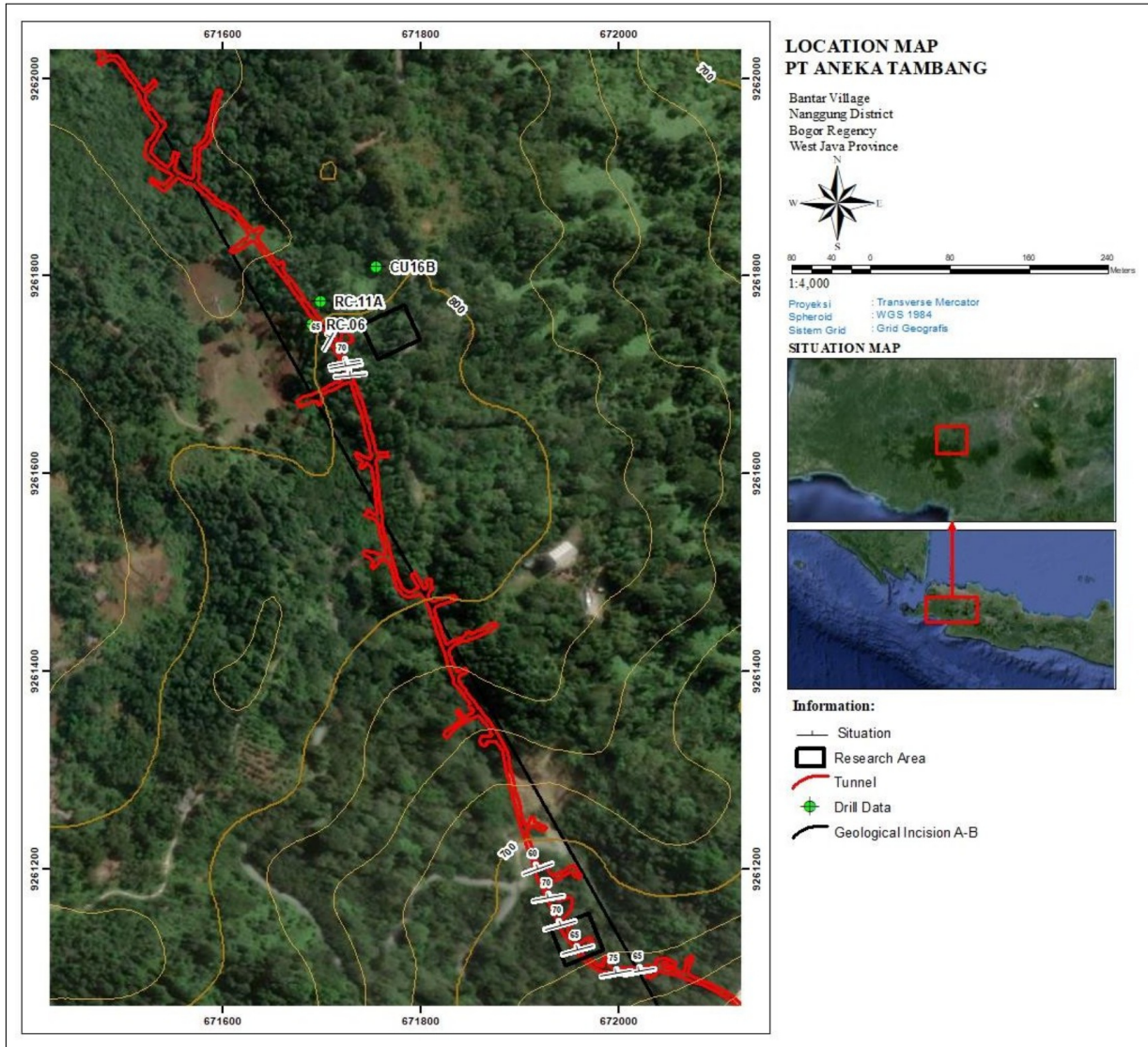


FIGURE 2. Ciurug route map of PT. Antam Pongkor.

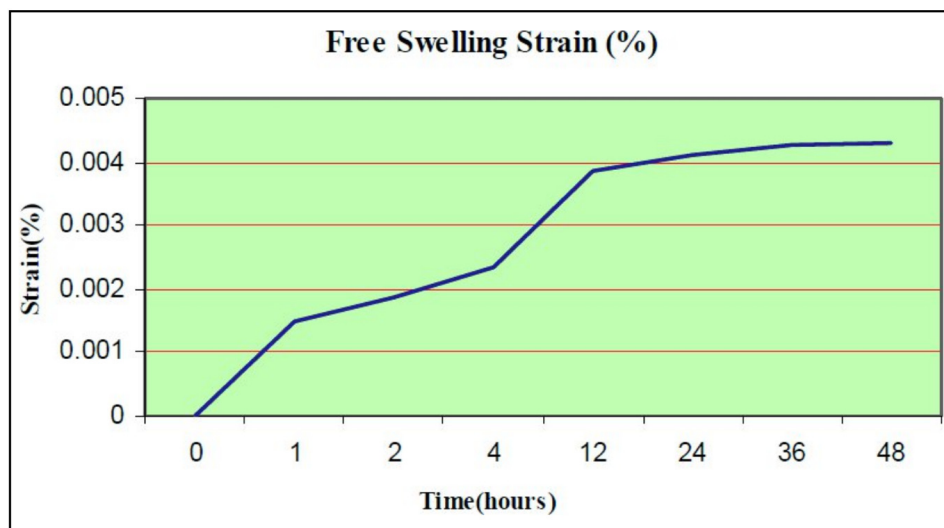


FIGURE 3. Strain experiment results in the free swelling test (Bayati *et al.*, 2021).

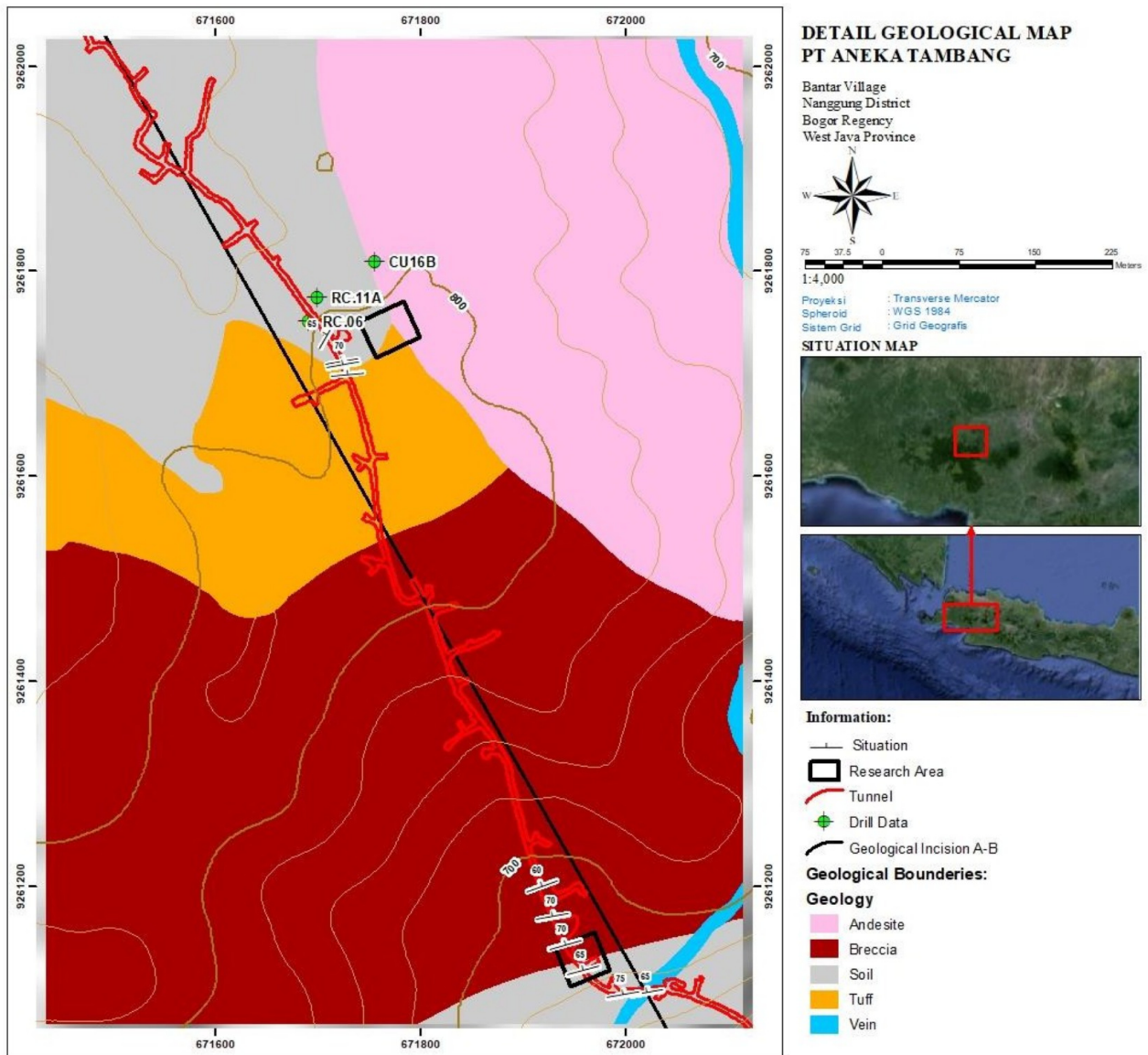


FIGURE 4. Detail geological map of the research location.

4.1 Lithology

Based on the geological map of PT. Antam Pongkor and survey of research locations, the lithology found on the surface of the underground mine consists of 3 types: tuff, breccia, and andesite. The research location is in XC Loop 2 and Unfoloader 600.

4.1.1 Unfoloader 600 location (tuff rock unit)

The Unfoloader 600 location has breccia and tuff rock units, tuff which, macroscopically this rock have not undergone changes or alteration (Figure 5). This rock has a fresh white color and a yellow-weathered color. The grain size is coarse dust (1/16–2 mm), the degree of roundness is semi-rounded to semi-angular, the sorting is good, and the packaging is closed. The composition of the rock consists of plagioclase, quartz, and volcanic glass.

4.1.2 Unfoloader 600 location (breccia rock unit)

The first rock found at the observation location is breccia, which has undergone megascopically changes or alteration (Figure 6). This rock was found after entering the Unfoloader 600. The fresh color is light grey, and the weathered color is dark grey; the structure is graded bedding, the grain size is clumpy (64–256 mm), the sorting is poor, the degree of roundness is semi-rounded to semi-angular, open-packed with fragments measuring 1–256 mm and a matrix of <0.1 mm.

There is a unit contact at the Unfoloader 600 location, namely the contact of the breccia rock unit with the Tuff rock unit that has undergone alteration. This observation was carried out megascopically (Figure 7).

4.1.3 XC loop 2 location (tuff rock unit)

The second tuff rock, which megascopically has undergone changes or alteration (Figure 8). This rock has a fresh yellowish-white color and a brownish-yellow weathered color. The grain size is coarse dust (1/16–2 mm), the degree of roundness is semi-rounded to semi-angular, the sorting is good, and the packaging is closed. The composition of the rock consists of plagioclase, quartz, sericite, and glass. There is a unit contact at the XC Loop 2 development location, namely the contact of andesite with Tuff that

has undergone alteration (glass material undergoes diagenesis into silica or silica oxide). This observation was carried out megascopically because the alteration process intensively causes the condition of the rock, so it is impossible to carry out.

4.1.4 XC loop 2 location (andesite rock unit)

The third rock found at the observation location is andesite, which has undergone megascopically changes or alteration (Figure 9). This rock was seen before entering the XC Loop 2 stop. This rock has a fresh grey color and a blackish-grey-weathered color. The structure is massive, the degree of crystallization is hypocrySTALLINE, the degree of granularity is porphyro-aphaneric (1–5 mm), and the crystal form is anhedral-subhedral. The mineral composition comprises plagioclase, chlorite, calcite, k-feldspar, quartz, pyroxene, and pyrite.

There is a unit contact at the development XC Loop 2 location, namely the contact of andesite rock units with tuff rock units that have undergone alteration (volcanic glass material undergoes diagenesis into silica or silica oxide). This observation was carried out megascopically (Figure 10).

4.2 Free swelling

The results of the free swelling analysis at the Unfoloader 600 Ciurug mine, with a depth of 650–700 meters below the surface, show the level of free swelling value is 102.94 % with 24 hours of testing, the justification for the expansion potential is very high (Figure 11). The results of the free swelling analysis at the XC Loop 2 Ciurug mine, with a depth of 650–700 meters below the surface, the level of free swelling value is 131.25 % with 24 hours of testing, the justification for the expansion potential is very high (Figure 12).

4.3 Clay mineralogy

XRD tests carried out the results of the free swelling test to determine the minerals contained in each research location of the underground mining development area.

4.3.1 Unfoloader 600

Based on the results of XRD analysis, the clay minerals present in the development area of the

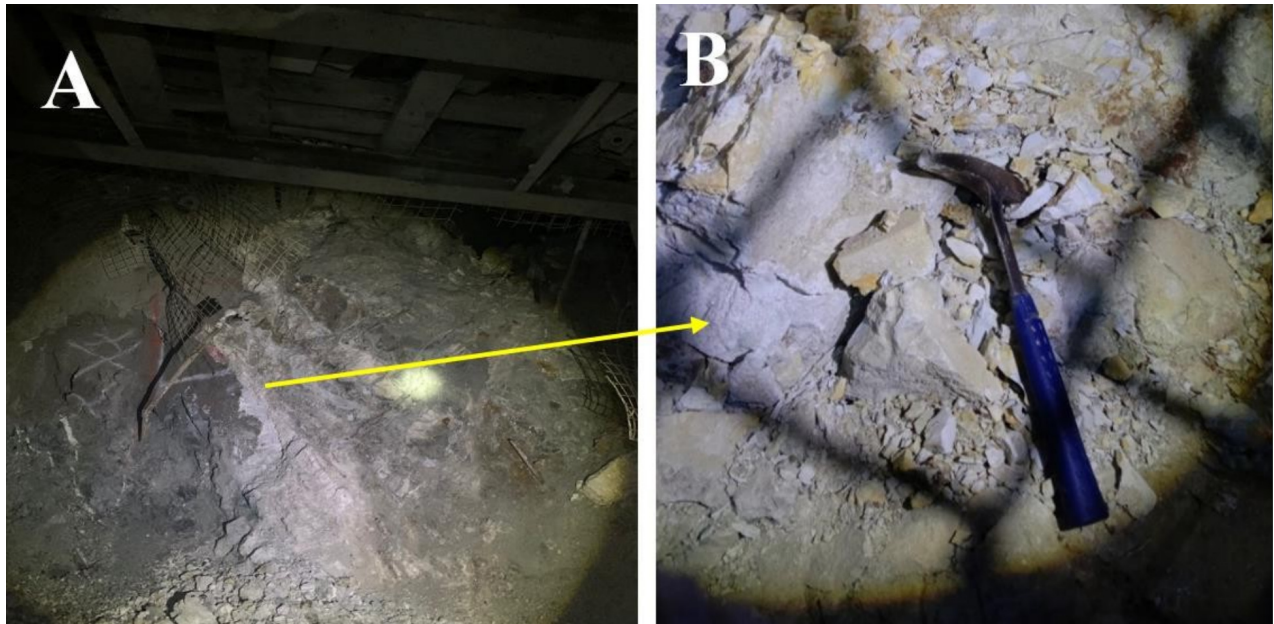


FIGURE 5. The megascopic appearance of tuff rock at the development of Unfoloader 600.

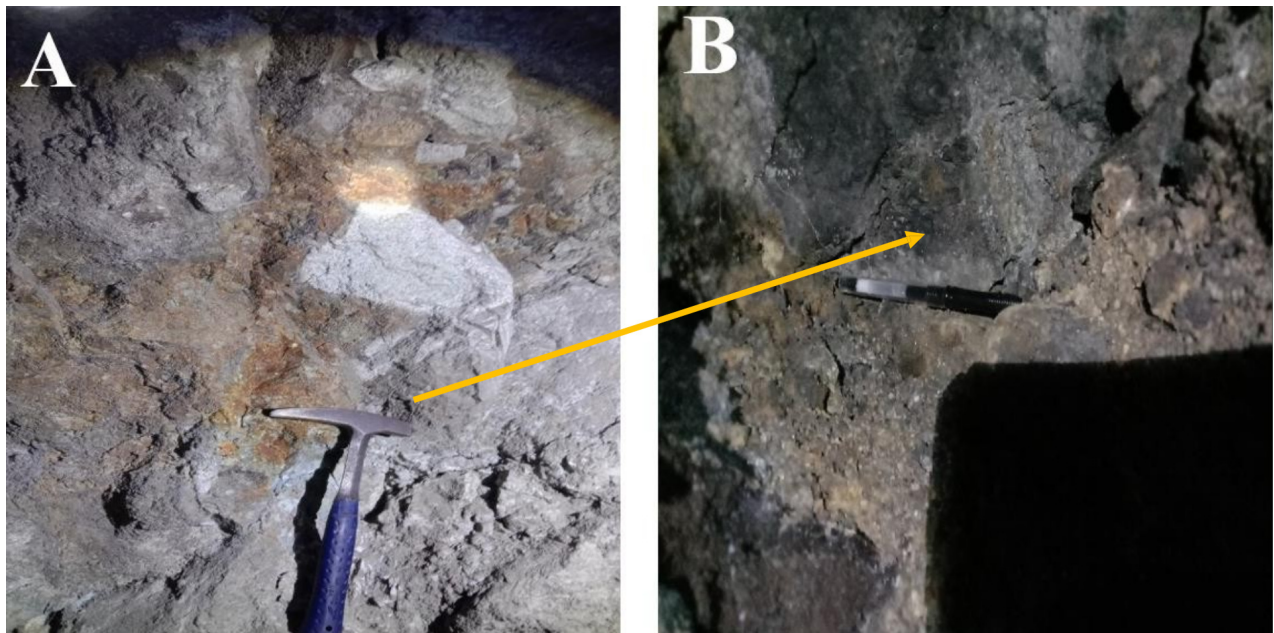


FIGURE 6. Breccia unit, the outcrop is located at Unfoloader 600.

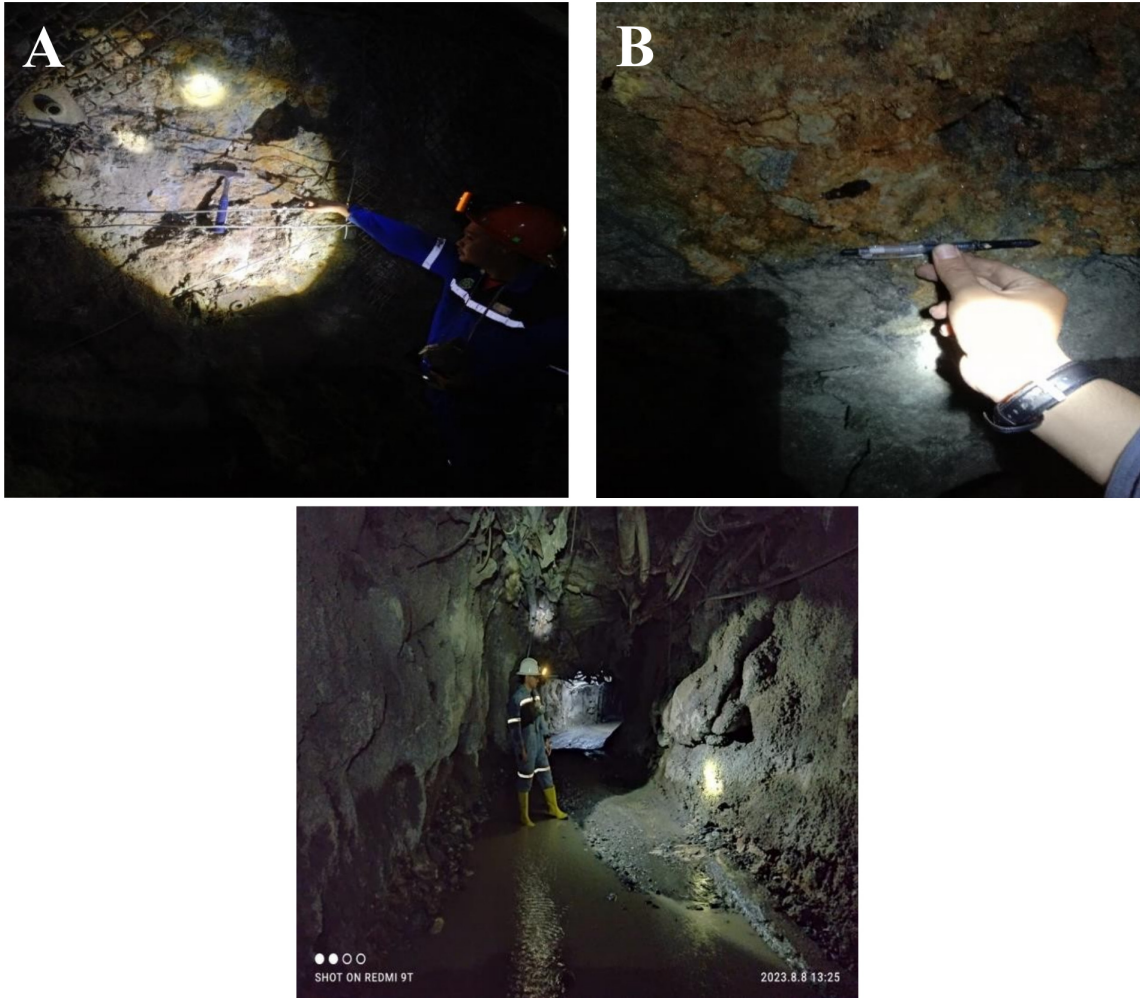


FIGURE 7. A. Long-range macroscopic view of the contact between breccia and tuff rock units. B. Close-up view of breccia and tuff rock units at the Unfolder 600 location and C. Actual conditions in the field at the Unfolder development location.



FIGURE 8. Tuff unit the research location is in XC Loop 2.



FIGURE 9. Andesite unit, the outcrop is located in XC Loop 2.



FIGURE 10. A. Long-range macroscopic appearance of contact between tuff and andesite rock units. B. Close-up appearance of Tuff and andesite rock units at XC Loop 2 and C. Actual conditions in the field at the development XC Loop 2 location.

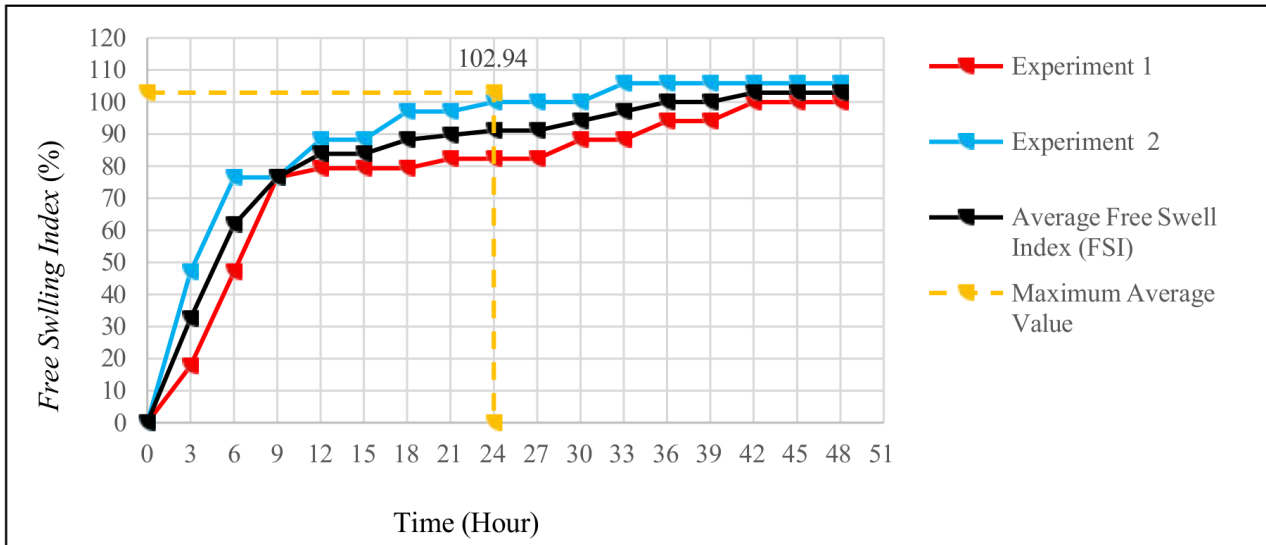


FIGURE 11. Results-free swelling test of Unfoloader 600 sample.

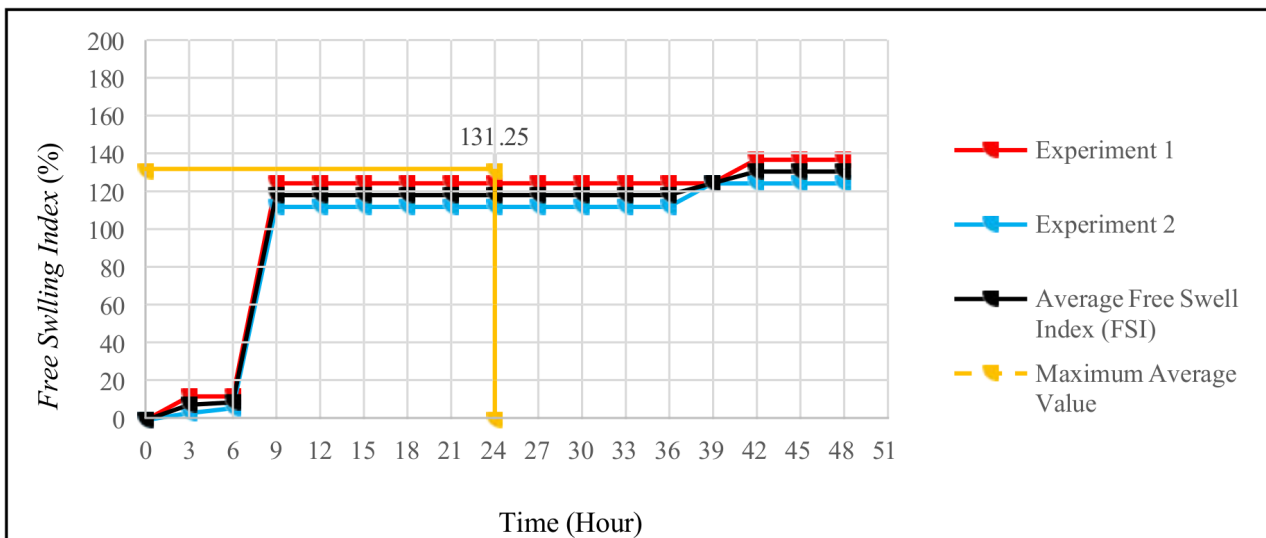


FIGURE 12. Results-free swelling test of XC Loop 2 sample.

Unfolder 600 location are illite, kaolinite, and montmorillonite. Figure 13 is the result of clay-dried sample analysis obtained from XRD testing in the laboratory. Figure 14 explains the results obtained from clay-dried sample testing of XRD test illite mineral composition of 21.9 %, kaolinite mineral composition of 75.1 %, and montmorillonite mineral composition of 2.9 %.

4.3.2 XC loop 2

Based on the results of XRD analysis, clay minerals are present in the development area of location Xc 600 loop 2. These are the minerals illite, kaolinite, and montmorillonite. Figure 15 is the result of clay-dried sample analysis obtained from XRD testing in the laboratory. Figure 16 explains the results obtained from the clay-dried sample testing of XRD from illite mineral composition of 83.6 %, kaolinite mineral composition of 13.3 %, and montmorillonite mineral composition of 3.1 %.

5 CONCLUSION

The conclusions that can be drawn based on the results of this study are as follows:

- a. The high level of development based on the results of the free swelling test at the openings of the XC Loop 2 development location was 131.25 % compared to the Unfolder 600 development location of 102.94 %.
- b. The presence of clay minerals based on the results of XRD testing at the Unfolder 600 and XC Loop 2 locations found clay minerals in the form of (illite, kaolinite, and montmorillonite) with varying percentages.

Acknowledgements The author would like to express his gratitude to Bagaskara Widi Nugroho, S.T., Suparjono, and Mukri as field supervisors at PT. Antam Pongkor has supported and allowed the author to take 2 locations as a place for thesis research.

REFERENCES

- Ashayeri, I., & Yasrebi, S. (2009). Free-Swell and Swelling Pressure of Unsaturated Compacted Clays; Experiments and Neural Networks Modeling. *Geotech. Geological Engineering*, 137-153.
- Barla, M. (1999). Tunnels in Swelling Ground: Simulation of 3D Stress Paths by Triaxial Laboratory Testing. Politecnico di Torino.
- Bayati, M., Taheri, A., Rasouli, V., & Saadat, M. (2021). A Numerical Approach to Simulate Stresses Around Tunnels In Swelling Rocks. *Geoengineering*, 15-22.
- Bunaciu, A., Udriștioiu, E.G., & Aboul-Enein, H.Y. (2015). X-Ray Diffraction: Instrumentation and Applications. *Critical Reviews in Analytical Chemistry*, v. 45, p. 289–299.
- Butscher, C., Einstein Herbert H., & Huggenberger, P. (2011). Effects of tunneling on groundwater flow and swelling of clay-sulfate rocks. *Water Resources Research*, 47, W11520, DOI: [10.1029/2011WR011023](https://doi.org/10.1029/2011WR011023).
- Das, B. (2010). Principles of Geotechnical Engineering Seventh Edition: America Cengage Learning, 1 26–34 73–80 p.
- Hoek, E., & Brown, E.T. (1982). Underground Excavation in Rock: London, E and FN Spon.
- Nelson, J., Chao, C., Overton, D., & Nelson, J., (2015). Foundation Engineering for Expansive Soils: Canada, John Wiley and Sons Inc, 30–39 31–32 p.
- Pirajno, F. (2009). Hydrothermal Processes and Mineral Systems, Geological Survey of Western Australia, Springer, Australia.
- Seed, H.B., Woodward R.J., & Lundgren. R., (1962). Prediction of swelling potential for compacted clays. *J Soil Mech Found. Div*, ASCE 88:53–87.
- Warmada, I.W, Lehmann, B., & Simandjuntak, M. (2003). Polymetallic sulfides and sulfosalts of the Pongkor epithermal gold-silver deposit, West Java, Indonesia. *The Canadian Mineralogist*, 41, pp. 185-200.
- Wesley, L.D. (2010). Soil Mechanics for Sedimentary and Residual Soils, ANDI, Yogyakarta.
- Wicaksono, D.D., Setiawan, N.I., Wilopo, W., & Harjoko, A., 2017, Sample Preparation Techniques in Mineralogical Analysis with XRD (X-Ray Diffraction) in the Department of Geological Engineering, Faculty of Engineering, Universitas Gajah Mada, in 10th National Seminar on Earth, p. 1864–1880.

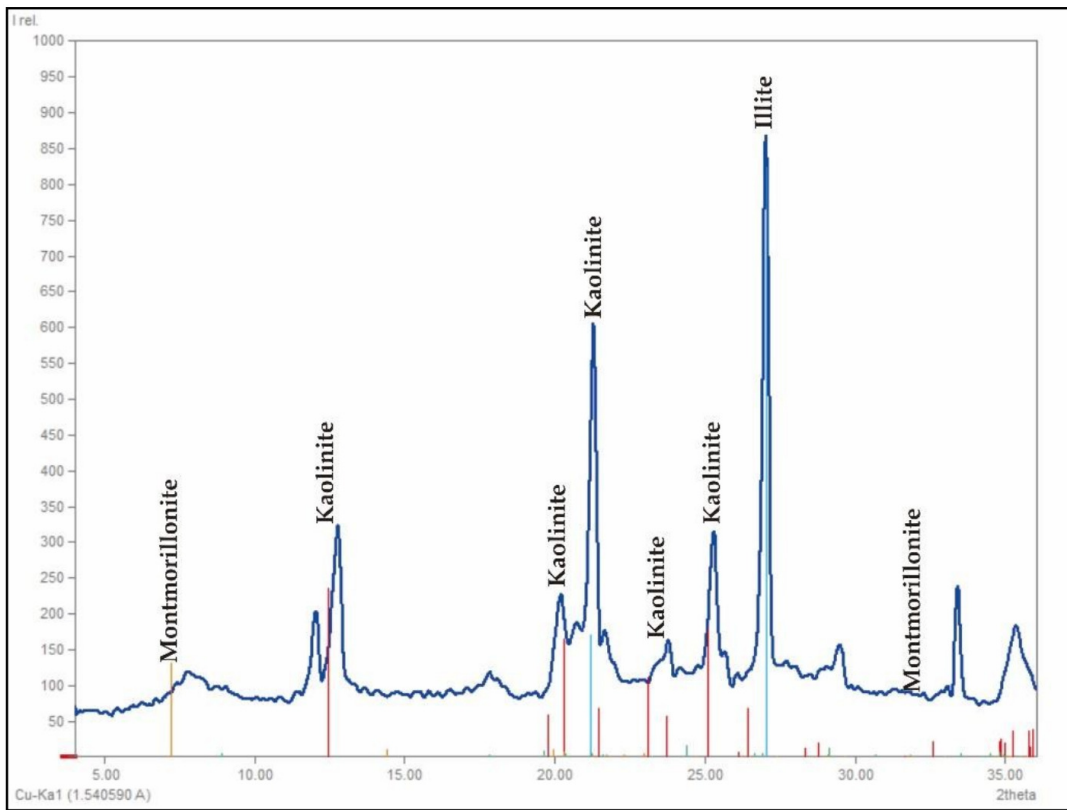


FIGURE 13. Test results of the Unfolder 600 sample.

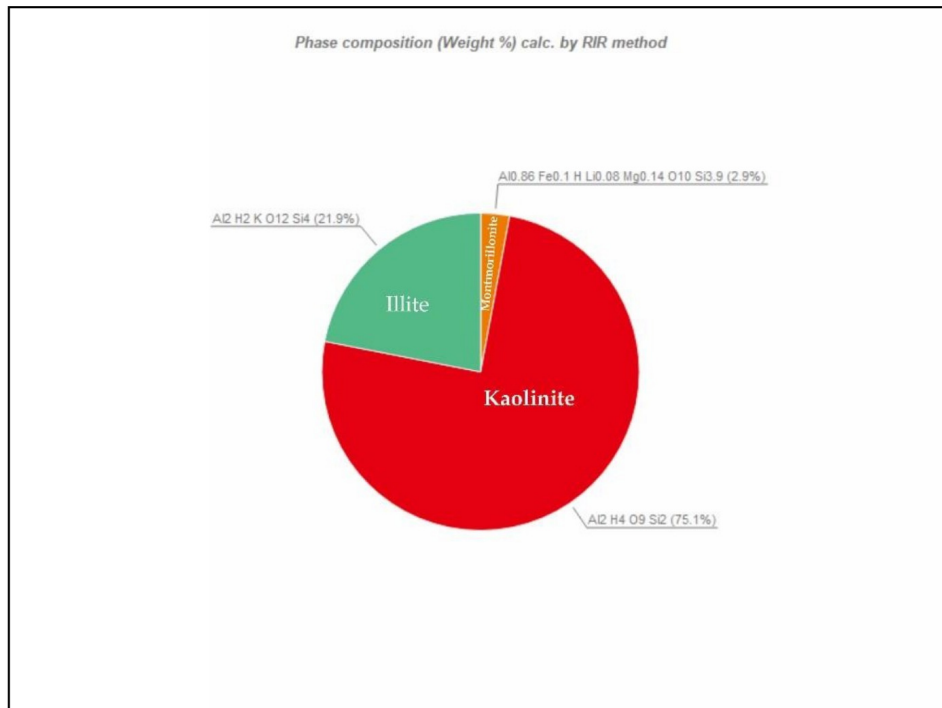


FIGURE 14. Percentage results of the Unfolder 600 sample.

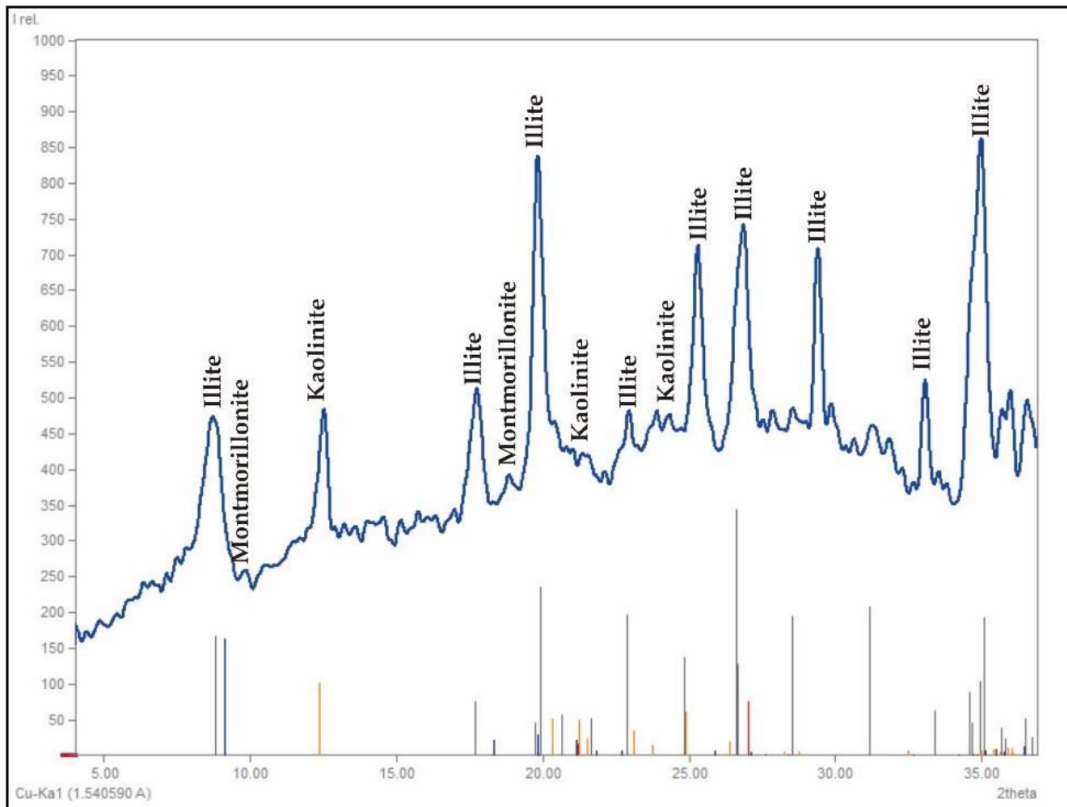


FIGURE 15. Test results of the XC Loop 2 sample.

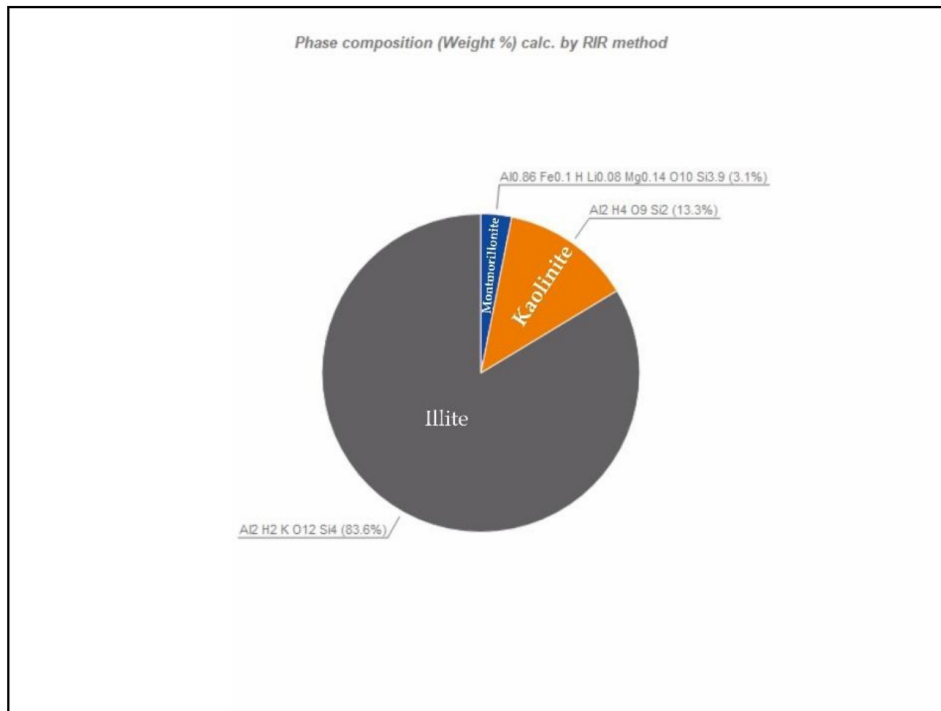


FIGURE 16. Percentage results of the XC Loop 2 sample.